https://doi.org/10.1016/j.buildenv.2020.106809

Development of a multi-nodal thermal regulation and comfort model for the outdoor environment assessment

Yongxin XIE[a], Jianlei Niu[a,*], Hui Zhang[b], Sijie Liu[c], Jianlin Liu[d], Taiyang Huang[a], Jianong Li[a], Cheuk Ming Mak[a]

[a] Department of Building Services Engineering, The Hong Kong Polytechnic University, Hunghom, Kowloon, Hong Kong
[b] Center for Built and Environment, University of California, Berkeley, CA 94720, USA
[c] School of Built Environment, The University of New South Wales, Sydney, Australia
[d] College of Environmental Science and Engineering, Donghua University, Shanghai, P. R. China
[*]*Corresponding email: bejlniu@polyu.edu.hk*

Abstract

The growing need for planning eco-cities is calling on a tool that can give better prediction of the thermal comfort conditions for a specific microclimate. A multi-nodal thermal regulation model can potentially factor in the impacts of the transient and asymmetric thermal conditions on human subjects. In this study, Human subjects were invited to experience various kinds of urban open spaces and to express their thermal feelings, while skin temperatures of 17 local body segments were measured. We tested the multi-nodal thermal regulation model developed by UC Berkeley by comparing its predictions of human body skin temperature, thermal sensation vote (TSV), and thermal comfort vote (TCV) with our onsite human subject measurements and questionnaire survey, in order to identify the causes of the errors between the prediction and measurements. Corresponding to the thermal neutral status, the field-measured data recorded wider local skin temperature ranges than the simulated ones. We proposed using a "null zone" instead of "set-point" in the thermal comfort model to accommodate the possible adaptation of human subjects to the highly fluctuating wind environment in open spaces. The forehead was suggested to be counted as one of the dominant local body parts when defining the overall thermal sensation. The correlation coefficient R^2 between the prediction and the field measured TSV improved to 93.7% for the revised model from 76.2% of the original model.

Keywords: outdoor thermal comfort; multi-nodal thermal regulation model; physiological parameters; null zone; set-point.

1 Introduction

Many cities worldwide have broken their hottest temperature records in the summer of 2019 [1]. As a highly urbanized city in the subtropical area, Hong Kong also had a record of 35.1 ℃ in summer 2019 (data obtained from the Hong Kong Observatory) (Fig. 1). The recorded highest day temperature in summer months has an increasing trend. The increasing occurrences of the extreme heatwave in the cities force the city planners to value more about the sustainable usage of urban open environment [2]. And thus, it is calling for a tool or an index for the accurate evaluation of the outdoor thermal comfort conditions, and give accurate evaluations

of the strategies for improving the urban thermal environment, such as increasing greenery [3, 4], creating shading area [5] and providing a windy environment for the pedestrians by rearranging urban geometry [6, 7].

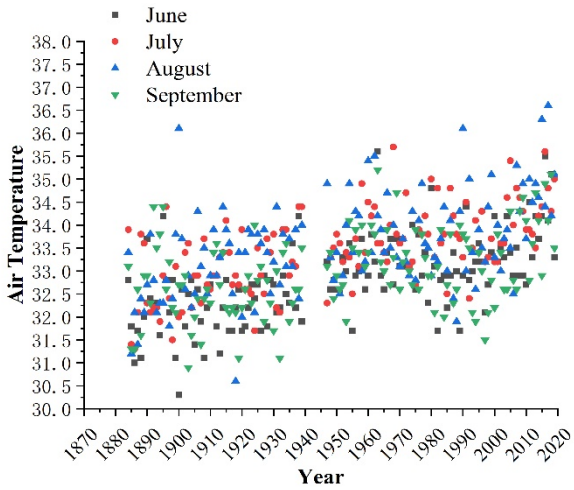

Fig. 1 The recorded highest day temperature in months from the year of 1884 to 2019 in Hong Kong

Researchers have devoted efforts in searching for a more precise index or tool to predict or evaluate thermal sensation and comfort for the urban microclimate [8, 9]. The thermal comfort models developed based on the multi-nodal model can potentially give more precise predictions when the unstable and asymmetric thermal environment is considered [10]. The models, such as the UTCI [11, 12] and the Berkeley Comfort Model (CBE model) [13-16], are now being tentatively used to evaluate outdoor environments [17-20]. CBE model provides a the comprehensive result of a 65-node thermal regulation model and a rational regression model developed from the human subject test under various thermal conditions created in the climate chamber [13, 14, 16]. The overall body thermal status as well as each weighted local thermal status on account of its strength of the local thermal sensation and its belonging body part (logic structure is shown in Appendix 1) [14]. Our preliminary study compared the prediction accuracy of thermal sensation from these models, it turned out that the CBE model gave more rational prediction compared with the UTCI model [19]. Still, some extreme prediction results were obtained in the warm-biased environment [19].

Thermoregulation aims at stabilizing the body temperature (T_b) with thermal sensation being its side product [21]. The Stolwijk 25-node model deeply rooted the control theory in thermoregulation models, including the CBE model [22]. “Load error” which triggers the regulatory processes is the soul of the control theory. “Set-point” is used as the reference temperature to calculate the load error, which serves as a feedback signal [23], to regulate the human body and to evaluate the thermal state [24]. The “load error” is defined as the deviation from the set-point of the regulated variable [25]. The warmth and cold thermoreceptors locate in different depths of the skin can sense thermal stimulation [26]. The activation of thermoreceptors depend on “load error” [27-29], and thus quantifying the deviation from the set-point has a direct effect on the intensity of thermal sensation perception. Therefore, the CBE

model defines “load error” for the perception of thermal sensation in a given local body part as the deviation of the actual local skin temperature and its local “set-point” [16]. The set-point for thermal sensation and comfort prediction of a given local body part is obtained in its thermal neutral status [15, 16]. Therefore, the particular concern should be given to the thermal neutral status.

Terms like “set-point" have been disputed for decades in thermal physiology. The original meaning of “set-point” comes from the engineering field and refers to an externally assigned physical reference signal in a unified control system. The term “set-point” has evoked much confusion for its usage in various situations: “set-point” is regarded as “the regulated body temperature of steady-state”; “the central reference signal” and “the thermal effector threshold” in the field of thermal physiology [30]. In the thermal comfort studies such as the Pierce model [31], the UTCI model [11], and the CBE model [15, 16], it is referred to the physiological parameters in its “thermal neutral status”. The controversy regarding such usage mainly comes from three aspects: the reference signal hypothesis, the unified entire system, the disturbance and acclimation. In recent years, the biologists and physiologists have come to an agreement that the reference signal hypothesis was untenable [21, 23, 32]. The last two usages, which are relevant to the topic discussing in this paper, will be briefly described below. The controversy in the aspect of the unified entire system comes from the field of thermal regulation, while the controversy in the aspect of the disturbance and acclimation comes from the thermal sensation and comfort studies.

The early research comparing the regulated variable with its set-point was a simplified explanation of the thermoregulation process in the human body [11, 24, 33]. However, such cognition would have to treat the human body as a unified entire system with a single controller or a single reference threshold, which has been proved as inappropriate and bringing in misunderstanding. Complex as the thermoregulation system in the human body, abundant thermoeffector loops exist [21], and their thresholds often change independently [21]. Furthermore, the integration of the responses to a particular external stimulation depends on abundant sensor-to-effector pathway connections [21]. Such complex interconnections through the central nervous system make it unlikely that any particular response is merely the outcome of one particular stimulus and thus requires some degree of variability or flexibility in temperature regulation [32].

As for the set-point related to the thermal neutral state, it is the value when the thermal balance is obtained, and the rate of heat storage is equal to zero [34]. “Set-point” here mainly refers to the “reference point” used in the thermal sensation and comfort models. If one strict value is considered without any variability, a slight change of the thermal environment could break the thermal neutral state corresponded to the given “set-point”, and thus changing thermal sensation correspondingly. It is barely impossible for the “steady state” or “thermal neutral state” to be established if the term “set-point” is considered [30], especially in the transient changing thermal environment. Moreover, the human body can adapt to a new steady level when persistent thermal disturbances happen. The balance of body temperature is further achieved in a new level due to the inherent property of dynamical stability of the thermoregulatory feedback

loop [30], thus shifting of thermal sensation response after adaption. Thermal adaptation is a higher level of control, on which either the heat transfer process or the thermoeffector properties (e.g., thresholds) are adjusted [35, 36], and hence a fixed "set-point" is not able to describe thermal adaption.

Therefore, how to handle the term "set-point" in the thermal sensation and comfort model is question worthy to be discussed, especially in the case of an urban open environment where unstable and asymmetric thermal stimulus becomes dominating. The existing CBE model has built a base structure that supports the change of "set-point" and has attempted to locate the adaptation thresholds [37]. However, the related datasets were too limited to establish the adaptation thresholds, and the datasets were obtained in the indoor setting where the transient thermal environment was created by step change of air temperature, and the complex wind environment in the outdoors could not be produced, which may be very different from the heat transfer mechanism and human response in the complex outdoor wind environment. Due to these factors, there is room for improvement if the CBE model is to be applied for the outdoor environment.

The aim of this paper is to develop the CBE model for the better prediction of thermal sensation in the outdoor environment. It will be achieved by first locating the source of prediction errors. Followed by a discussion between "null-zone" and "set-point". The "null-zone" range of local skin temperatures will be provided for the outdoor settings. Finally, the CBE model will be modified to fit the outdoor thermal characteristics.

2 Methods

2.1 On-site data collection

The on-site measurement was conducted from November 2017 to September 2018. The real-time meteorological data was collected by a micro-climate station. The technical information is listed in Table 1. The skin temperature of 17 local body parts was continuously collected. The skin temperature of local body parts such as pelvis, back, left foot, and right foot, which was not sensitive to slight thermal stimulations and covered by clothing, were collected using the i-buttons. The starting time, ending time and logging interval of each i-button were preset through a commercial software, OneWireViewer, before the experiment. Only temperature data will be collected. The other local body parts were measured using a thermocouple or thermal resistance with a portable data logger. The skin temperature measurement sites are shown in Fig 2. The data-logging interval for the skin temperature was 1 second. Detailed information about the skin temperature sensors is listed in Table 1.

Table. 1 Technical information on experimental equipment

Measured parameters	**Sensor/Equipment**	**Range of measurement**	**Accuracy**
Air temperature (Ta)	RM 41382	-50~50 ℃	±0.3 ℃
Relative humidity (RH)		0~100 %	±1 %
Wind speed (v)	R.M. YOUNG 81000	0~40 m/s	±0.05 m/s

Long-wave radiation ($\boldsymbol{Q_l}$)	Kipp & Zonen CNR-4	-250~250 W	<10%
Short-wave radiation ($\boldsymbol{Q_s}$)		0~2000 W	<5 %
Skin temperature	i-button (DS1922L)	-40~+85 ℃	±0.5 ℃
	TT-T-30-SLE (sensor)	-200~ 150 ℃	± (0.4 % or 0.5 ℃)
	BTM 4208 SD (data logger)	-50~ 400 ℃	± (0.4 % or 0.5 ℃)
	DataTaker DT 80 (data logger)	-270~+400 ℃	±0.1%
	TianJianHuaYi WZY-1	-20~80 ℃	±0.3 ℃

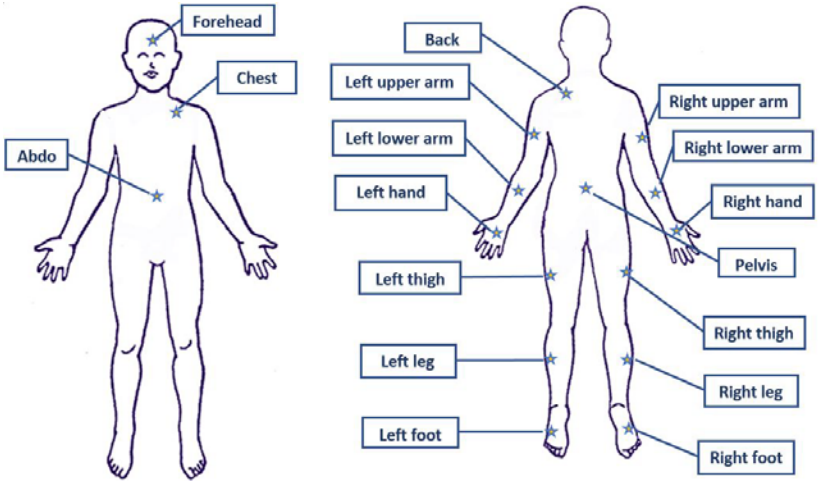

Fig. 2 Measurement points of local skin temperatures

The data was collected from two cities, Hong Kong and Sydney. The experiment conducted on the campus of Hong Kong Polytechnic University belonged to the transitional seasons and hot summer, while the winter experiments were conducted on the campus of the University of Sydney. Both experimental sites were surrounded by academic buildings with external wall material of red brick (approximate albedo is 0.3) [38] or glass curtain wall (the external reflectance (ER_{Glass}) in Hong Kong should be no more than 0.2 according to the Design and Construction Requirements for Energy Efficiency of Residential Buildings in Hong Kong (APP-156) [39]). The pavement material for the sites were grass (approximate albedo is 0.2) [38] and concrete (approximate albedo is 0.225) [38] for Sydney and Hong Kong respectively.

The human subjects were required to wear regular clothing suitable to the weather to join the experiment. In total, 531 survey responses were collected during the whole year, 428 survey responses were available along with the measured skin temperature dataset after removing the missing data and limiting the activity level to sit or stand only. Within the available datasets, altogether 42 males (35 in Hong Kong and 7 in Sydney) and 32 females (28 in Hong Kong and 4 in Sydney) joined the experiment. Only the students and young colleges from China were

invited to join the experiment to avoid differences in thermal feelings caused by culture differences. About 30 minutes were allowed before the start of the experiment to attach the sensor and to stabilize the transient metabolic rate. During the experiment, the human subjects were required to sit or stand, experience the specific outdoor thermal environment, and fill in the survey. Fig. 3 shows two examples of experiment setup on two campuses. The microclimate stations used on two campuses were of the same type.

Fig. 3 Experiment photo (left) Sydney; (right) Hong Kong

The survey focused on the perception of local and overall thermal sensation and thermal comfort, along with the collection of individual information (gender, age, height, weight, and clothing information). Ethical approval was obtained in both universities, and the collected data was for research usage only. Each human subject experienced a specific outdoor environment for about 40 minutes and filled in the survey every 5 minute. An extended nine-point scale was adopted to evaluate the subject's thermal sensation and thermal comfort [40].

2.2 Direct and diffuse solar radiation

One of the main differences between the thermal environment of the indoors and the outdoors comes from radiation. The primary source of radiation in the indoor environment comes from long-wave irradiation; whereas, short-wave irradiation is the primary radiation source in the urban open space [41]. Meanwhile, long-wave irradiation cannot be neglected given the heat absorbed by the surroundings in the urban setting. Short-wave irradiation includes both the direct and diffuse solar irradiation [41]. The pyranometer from CNR-4 gives the data of short-wave irradiation while the pyrgeometer gives the information related to long-wave irradiation. The input of long-wave irradiation in the CBE model will follow the method described in our earlier publication [19].The subject placed in the center of an imaginary enclosed room with different equivalent surface temperature from six walls was created in the CBE model [19]. The radiometer was assumed to be at the center of the imaginary room. The long-wave irradiation collected by the pyrgeometers facing six directions were used to calculate the equivalent surface temperature of six walls by repeating the method described in Equation 1 [19].

$$T_{mrt-i}^4 = T_{s1}^4 F_{i-s1} + T_{s2}^4 F_{i-s2} + T_{s3}^4 F_{i-s3} + T_{s4}^4 F_{i-s4} + T_{s5}^4 F_{i-s5} + T_{s6}^4 F_{i-s6} \quad \text{Equation (1)}$$

The short-wave irradiation will be separated as direct and diffuse irradiation. The upward and downward facing CNR 4 pyranometers were able to collect the incoming shortwave irradiation and the reflected shortwave irradiation in 180 degree respectively [42]. The average near-ground albedo is calculated by the ratio of incoming and reflected solar radiation measured by a pair of horizontally placed pyranometers in the standing height of pedestrian (Equation 1) [41]. Therefore, the average near-ground albedo represents the approximate ratio of reflected solar radiation by the opaque surfaces and objects in standing height of pedestrian. The global horizontal irradiance (GHI) was measured by the horizontal pyranometer facing the sky, while the global tilted irradiance (GTI) was measured by the north-facing pyranometer. When the surface is tilted to the horizontal, the total irradiance comes from three aspects, which are the incident diffuse radiation on the tilted surface, the direct normal irradiance projected onto the tilted surface, and the near-ground reflected irradiance that is incident on the tilted surface [41]. The diffuse radiation received by a tilted surface adopts the simplest isotropic diffuse model (Equation 4) [43, 44]. The reflected radiation received by the tilted surface is difficult to accurately model because of the inhomogeneous distribution of opaque objects near ground. Here, a simple isotropic model is adopted to estimate the reflected solar radiation in standing height (Equation 4) [41]. By combining the measurement results facing the North and the sky together, DHI (direct normal irradiance) and DNI (diffuse horizontal irradiance) can be solved using the listed equations 2-6 [41] below and then as the inputs in the CBE model.

$$\rho = GHI_{lower}/GHI_{upper} \quad \text{Equation (2)}$$

$$sza = 90° - elv \quad \text{Equation (3)}$$

$$GHI_{upper} = DNI \cdot cos(sza) + DHI \quad \text{Equation (4)}$$

$$cos(sza_r) = cos(T) \cdot cos(sza) + sin(T) \cdot sin(sza) \cdot cos(az - \gamma) \quad \text{Equation (5)}$$

$$GTI = DNI \cdot cos(sza_r) + DHI \cdot (1 + cos(T))/2 + GHI \cdot \rho \cdot (1 - cos(T))/2 \quad \text{Equation (6)}$$

where:

ρ: the average near-ground albedo;

az: the azimuth angle;

elv: the elevation angle, measured from the horizon to the solar position;

γ: the surface is rotated by γ degrees (with north-facing being $90°$ and upper-facing being zero);

T: the surface is tilted by T degrees (with north-facing being $90°$ and upper-facing being zero);

sza: the solar zenith angle, measured from the vertical to the solar position;

sza_r: the angle of incidence of the DNI to the tilted surface;

DHI: the direct normal irradiance;

DNI: the diffuse horizontal irradiance;

GHI: the global horizontal irradiance.

GHI_{lower}: the global horizontal irradiance received by the pyranometers facing ground;
GHI_{upper}: the global horizontal irradiance received by the pyranometers facing the sky.
GTI: the global tilted irradiance on a surface with a given tilt and azimuth orientation;

3 Results and discussions

3.1 General description of the microclimate conditions

All the microclimate conditions in the available dataset is shown in Table 2. For the winter experiment in Sydney, T_a (air temperature) was in the range of 15.5 to 21.9 ℃ and T_{mrt} (mean radiant temperature) was in the range of 15.8 to 56.3 ℃. The ν (wind speed) was in the range of 0.4 to 2.2 m/s. Wind blew from the central Australia makes the winter in Sydney very dry, and the *RH* (relative humidity) was between 20.8 to 69.7%.

We also had limited winter experiment samples from Hong Kong, which covered the T_a range of 16.8 to 19.8 ℃. The dataset from transitional seasons and summer recorded the T_a range of 23.6 to 33.2 ℃. The T_{mrt} was from 16.9 to 57.6 ℃ while ν was from 0.1 to 4.6 m/s. The RH was from 31.9% to 78.4%. The distribution of T_{mrt} was either very closed to T_a (heavy cloudy day) or at its extreme high level (cloudless day), which explains the high level of standard deviation. The partly sunny or partly cloudy conditions were limited in our dataset. The mean wind speed in the experiment of Hong Kong was recorded in a wider range than that in Sydney, with twice the standard deviation than Sydney. Still, above 90% of the observed cases in Hong Kong concentrated below 2.14 m/s.

Table. 2 The microclimate condition distribution of experiment

Location	Hong Kong				Sydney			
	Mean	Max	Min	Standard deviation	Mean	Max	Min	Standard deviation
Air temperature (T_a, ℃)	26.7	33.2	16.8	2.9	18.7	21.9	15.5	1.9
Mean radiant temperature (T_{mrt}, ℃)	31.5	57.6	16.9	9.8	41.6	56.3	15.8	13.0
Wind speed (ν, m/s)	1.0	4.6	0.1	0.8	1.1	2.2	0.4	0.4
Relative humidity (Rh, %)	63.9	78.4	31.9	8.4	36.7	69.7	20.8	14.4

3.2 Primary comparison of the field data and the simulated data

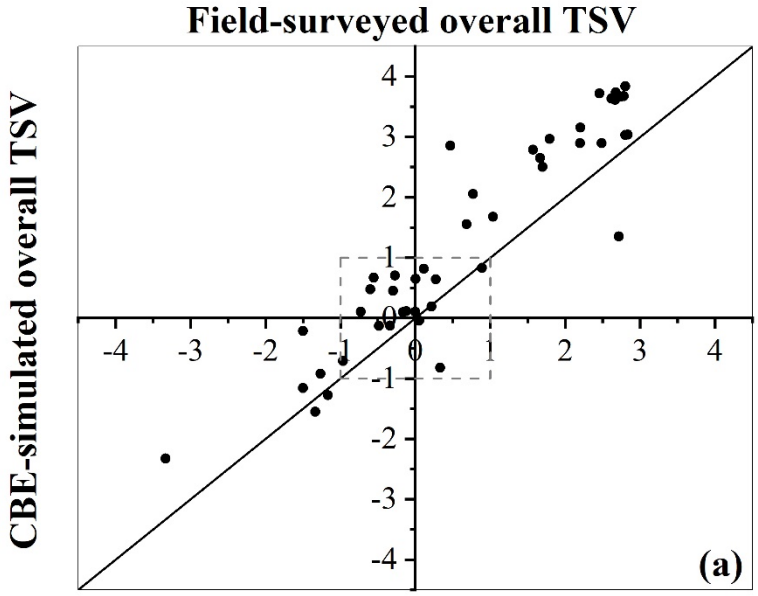

285

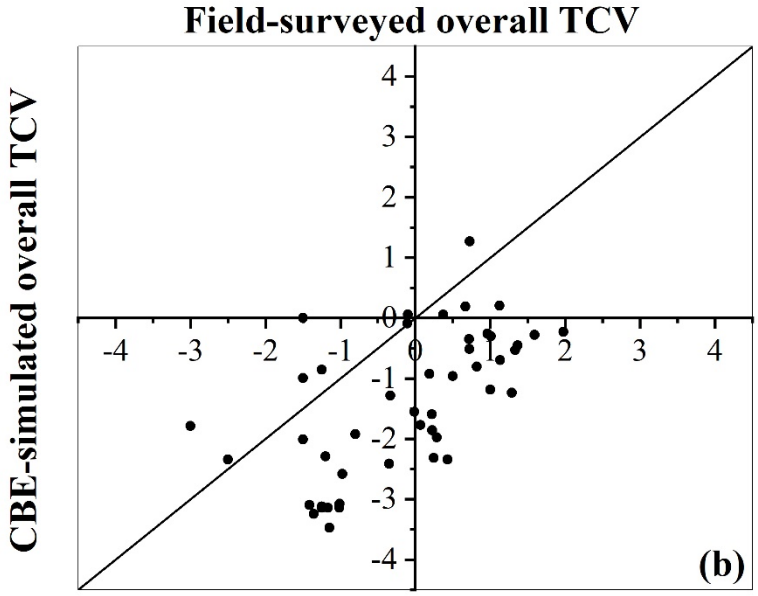

286

287 Fig. 4 The relation between the field surveyed and simulated: (a) thermal sensation vote
288 (TSV); (b) thermal comfort votes (TCV). (*The simulated TSV and TCV data were obtained
289 by using the measured environmental parameters, and the surveyed subject personal data
290 (such as gender, weight, height, age and clothing pattern) as inputs.)
291

The data comparison between the field-surveyed data, and the simulated data will be started with the primary comparison of the overall TSV (thermal sensation vote) and TCV (thermal comfort vote). The simulated results in Fig. 4 were obtained from the original CBE software using the meteorological parameters and personal information of human subjects as input. Therefore, the simulated results in Fig. 4 are the comprehensive product of the 65-node thermoregulation model and the CBE comfort model. As an integrated environmental parameter, the operative temperature (T_{op}) was chosen as the representative to make the primary comparison. Each point shown in Fig. 4 was the average result based on T_{op}. The T_{op} covered the range of 15.7 to 45.7 ℃. The T_{op} in both the winter of Sydney and Hong Kong were mild, the cases of below 20.0 ℃ were limited. Therefore, only minimal data points are located in the lower extreme level of field-surveyed thermal sensation. The following analysis will be focused on the dataset of transitional seasons and summer.

Our previous study has proved that thermal neutral status does not equivalent to "TSV = 0" through the independent t-test of comparing a field-surveyed dataset and a randomly generated dataset [40]. The field-surveyed dataset in our previous study consisted of more than one thousand samples while the randomly generated dataset was constructed by the original field-surveyed data outside the range of [-1, 1] and the random integer values from -1 to 1 replacing the data in the range of [-1, 1] [40]. The statistic results show that people make no distinction among the categories of "slightly cool", "neutral" and "slightly warm" [40]. In other words, people who stayed in the outdoor environment tended to vote from "slightly cool" to "slightly warm" in their thermal neutrality [40]. This finding provides us the evidence to define "TSV = -1" and "TSV = 1" also as thermal neutral status when an integer is used as the survey input. Though the CBE model generates continuous voting, this study used the same range in defining thermal neutrality to unify the criteria for comparison.

Fig. 4 shows the comparison results of the thermal sensation vote. The simulated data points locate almost above the 45-degree line, indicating that the simulated data are higher than the field-surveyed data covering the whole range. In the thermal neutral status, almost all the simulated data located in the TSV > 0 side when the field-surveyed data voted in the range of [-1,1]. Extreme simulated data points existed when the field-surveyed data was in the range of [0,1].

From the aspect of thermal comfort (Fig.4 (b)), the CBE-simulated TCV was calculated in the stable phase. The rule of calculating overall TCV in a transient environment [14] was not applied here. Because the transient thermal environment mentioned in most of the thermal comfort studies refers to the case of transient changing of temperature, which is not applicable to our case. Regarding the wind environment, if wind speed keeps fluctuating in a limited range (no gust wind happens), such a case is referred to as enhanced convective heat transfer but not transient thermal environment. Furthermore, the existing studies are not able to describe the convective heat transfer effect of the outdoor wind environment due to limited experiment results in high turbulent intensity, needless to mention the transient effect by gust wind [45]. The wind tunnel experiment from Yu et al. [46] have confirmed that stronger heat transfer process existed under high turbulence intensity level. Therefore, we remained using the TCV

results in a stable phase for comparison. The field survey results had more than half of the points located on the comfort side. Most of the surveyed responses located on the uncomfortable side were quite close to “TCV = -1”, which corresponded to “slightly uncomfortable”. More data points located on the comfortable side than in the thermal neutral zone, meaning people still feel thermally comfortable even when the thermal sensation status is slightly away from the thermal neutrality in the outdoor environment. Compared with the field-surveyed results, most of the CBE-simulated results located on the uncomfortable side, and some were closed to the lower extremity.

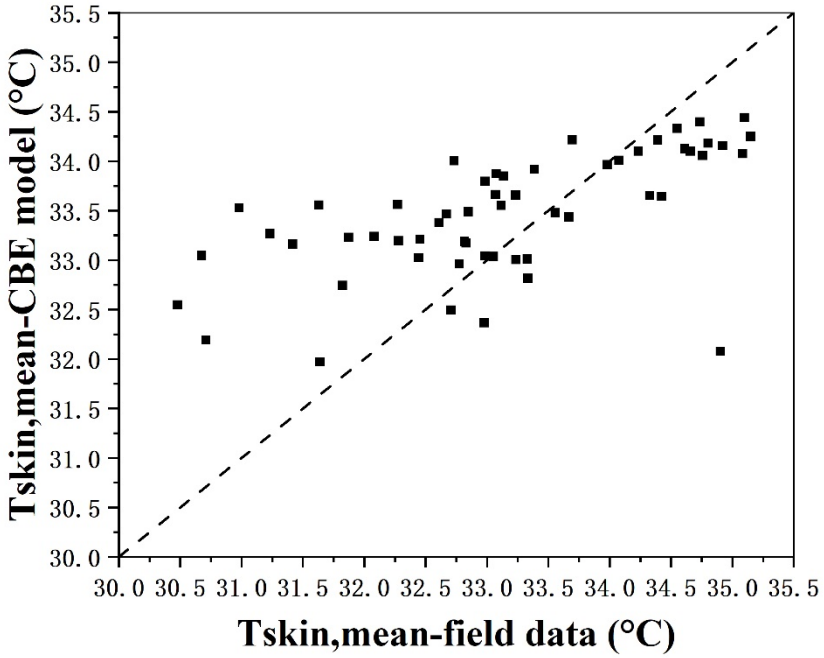

Fig. 5 Comparison between the measured and simulated mean skin temperatures ($T_{skin,m}$)

The comparison results of field measured, and CBE-simulated $T_{skin,m}$ (mean skin temperature) are shown in Fig. 5. The CBE-simulated mean skin temperature was the simulation results of the multi-nodal thermal regulation model based on the meteorological parameters. The CBE dataset was well reported by other researchers of having higher predictive value than their datasets [47, 48]. However, from our comparison results, the measured and simulated $T_{skin,m}$ were similar in the range of 32.5 and 34.0 ℃. The measured $T_{skin,m}$ was much lower than the simulated data when lower than 32.5 ℃ and higher than the simulated data when higher than 34.0 ℃. The results here show that the prediction gap exists between the multi-nodal thermal regulation model and the field-measured data. The main difference exists in the cold case. We compared our results with that from the mild cases conducted in the outdoor environment of Tianjin listed in the study of Lai et al. [49], within which the mild cases refer to T_a from 13.8 to 22.3 ℃ with the average solar radiation of 226.8 W/m^2. The meteorological conditions of the mild cases in Tianjin was similar to our experiment conditions in winter. The measured $T_{skin,m}$ from their study in the mild case was from 30.5 to 32.0 ℃ [49], which was similar

with our measurement results in the winter and supported the accuracy of our measurement results. We intended to use T_{skin} as the bridge to link the meteorological parameters and the thermal sensation response. The measured skin temperature will be the input parameters in the CBE comfort model instead of the collected meteorological parameters to avoid the prediction difference generated by the multi-nodal thermal regulation model.

3.3 Comparison of the thermal sensation based on local and mean skin temperatures

This part will focus on the comparison of the field-measured, and the CBE-simulated thermal sensation votes, both the local and overall TSV will be discussed (shown in Fig.6 (a-h)). The CBE-simulated TSV, including the local TSV and the overall TSV (Fig.6 (a-h)), were generated using the measured skin temperature as input to the CBE comfort model. The CBE comfort model was reproduced using Matlab based on the original logic, set-points, and the listed coefficients from the previous publications [13-16]. The updates of the model detail were also addressed [34]. The reproduced CBE comfort model was validated using the simulated datasets from the original CBE comfort software. The relation between the overall TSV and $T_{skin,m}$ (mean skin temperature) will be discussed along with the local TSV of seven body parts used in the calculation of $T_{skin,m}$ [37]. The mean skin temperature was calculated using the 7-point method, the same as which used in the CBE model [37]. The seven local body parts used in the 7-point method, such as forehead, abdomen, left lower arm, left hand, left upper leg, left lower leg, and left foot were included in the analysis.

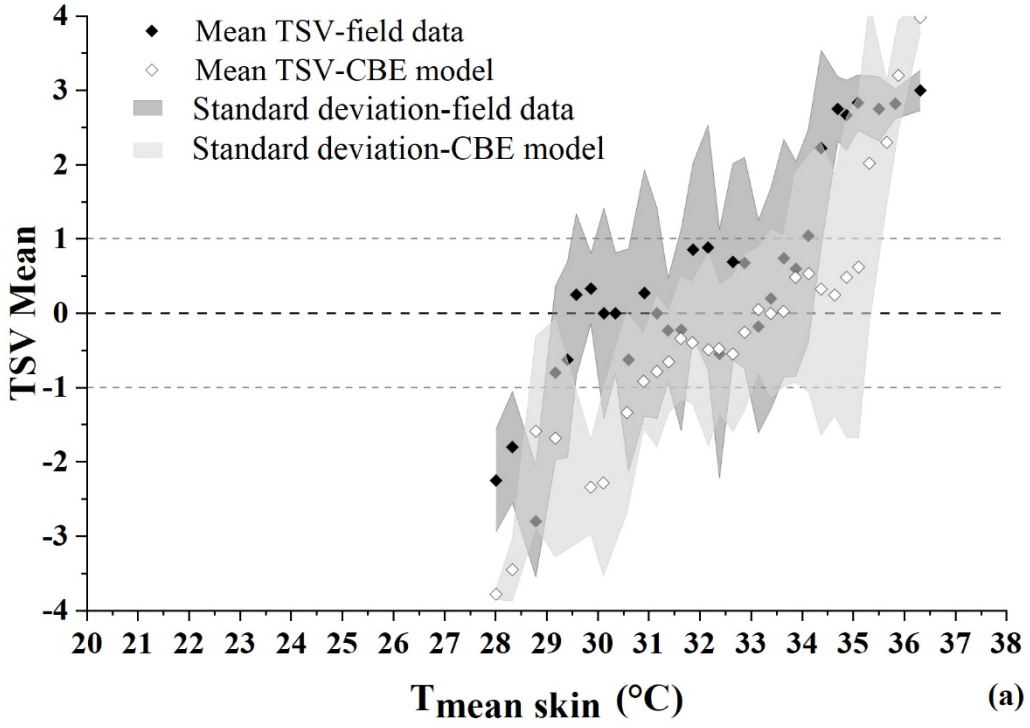

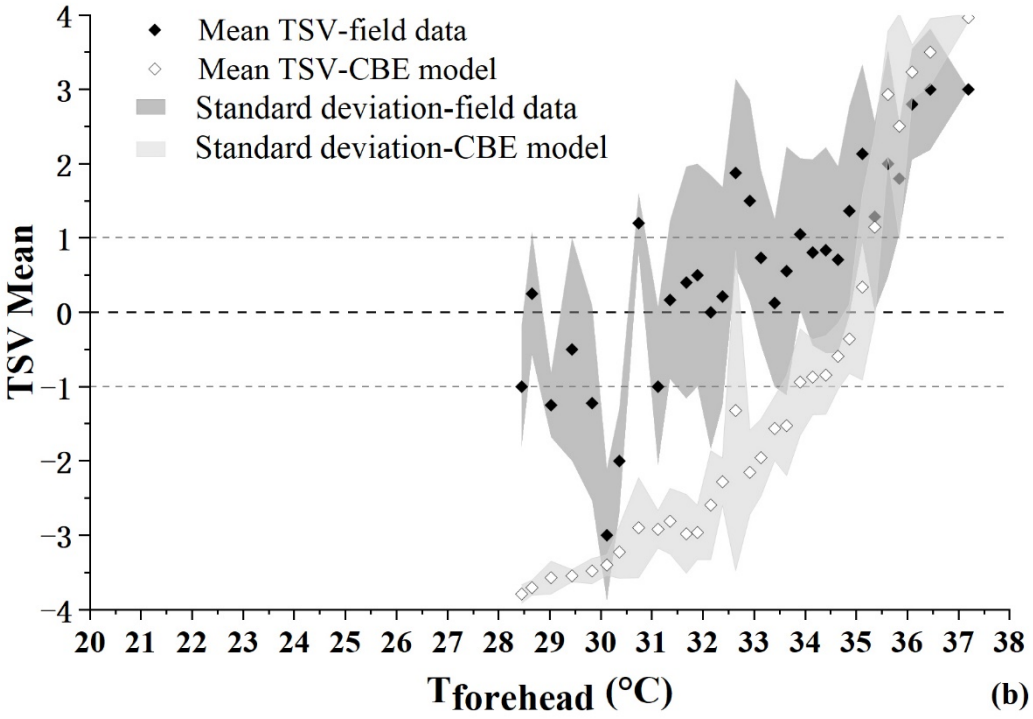
Mean TSV-field data
Mean TSV-CBE model
Standard deviation-field data
Standard deviation-CBE model
TSV Mean
4
3
2
1
0
−1
−2
−3
−4
20 21 22 23 24 25 26 27 28 29 30 31 32 33 34 35 36 37 38
Tforehead (°C)
(b)

384

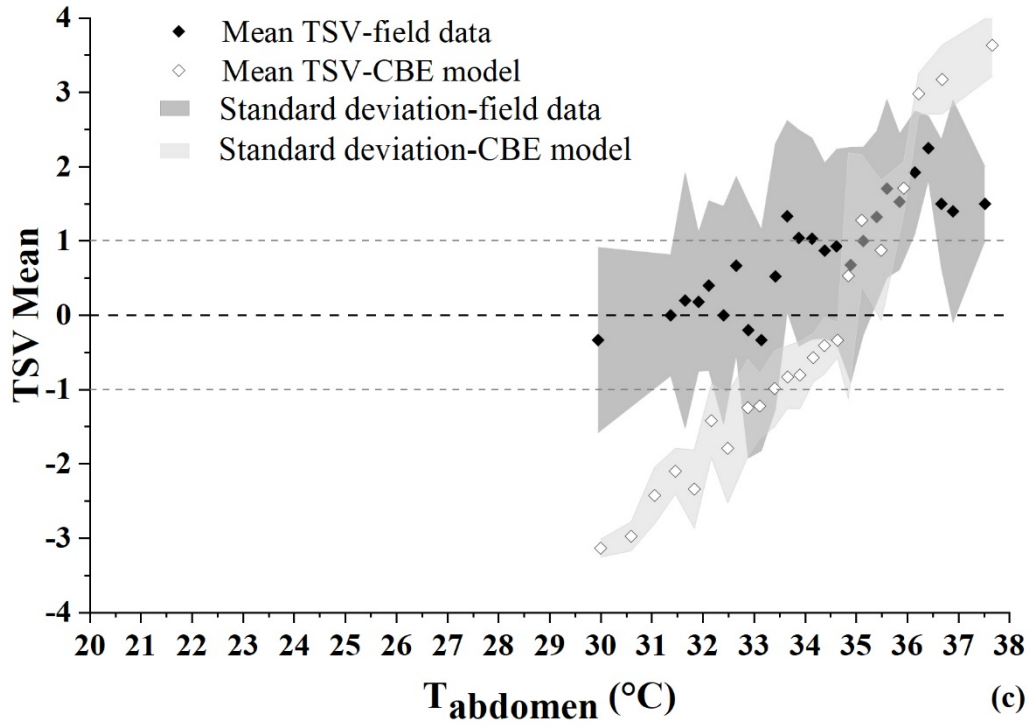
Mean TSV-field data
Mean TSV-CBE model
Standard deviation-field data
Standard deviation-CBE model
TSV Mean
4
3
2
1
0
-1
-2
-3
-4
20 21 22 23 24 25 26 27 28 29 30 31 32 33 34 35 36 37 38
Tabdomen (°C)
(c)

385

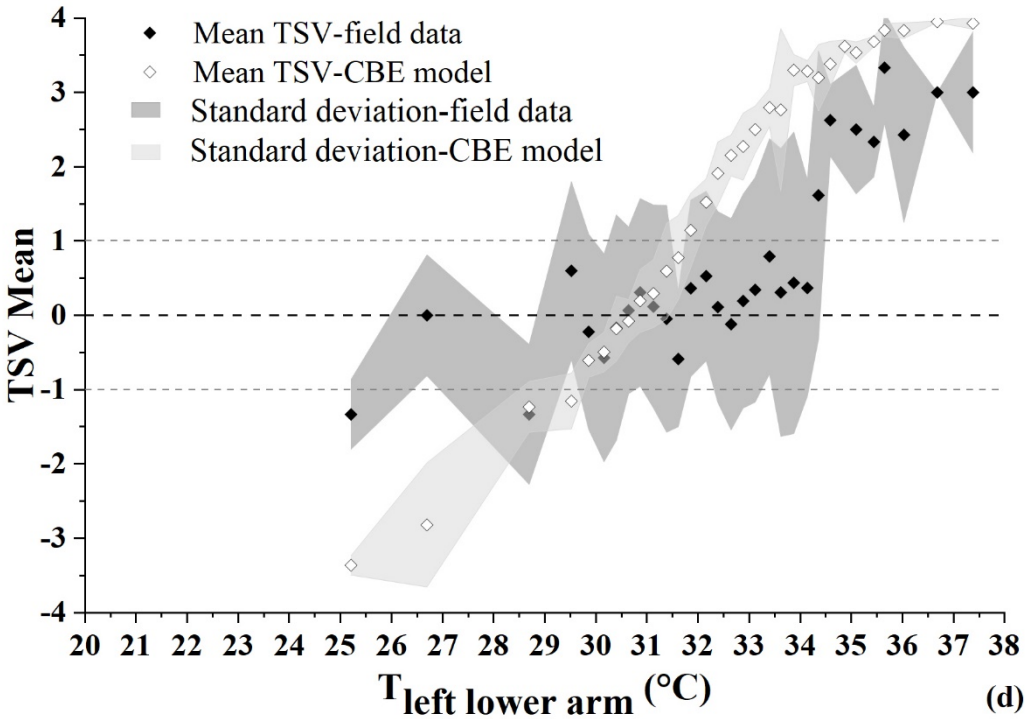
Mean TSV-field data
Mean TSV-CBE model
Standard deviation-field data
Standard deviation-CBE model
TSV Mean
4
3
2
1
0
-1
-2
-3
-4
20 21 22 23 24 25 26 27 28 29 30 31 32 33 34 35 36 37 38
T left lower arm (°C)
(d)

386

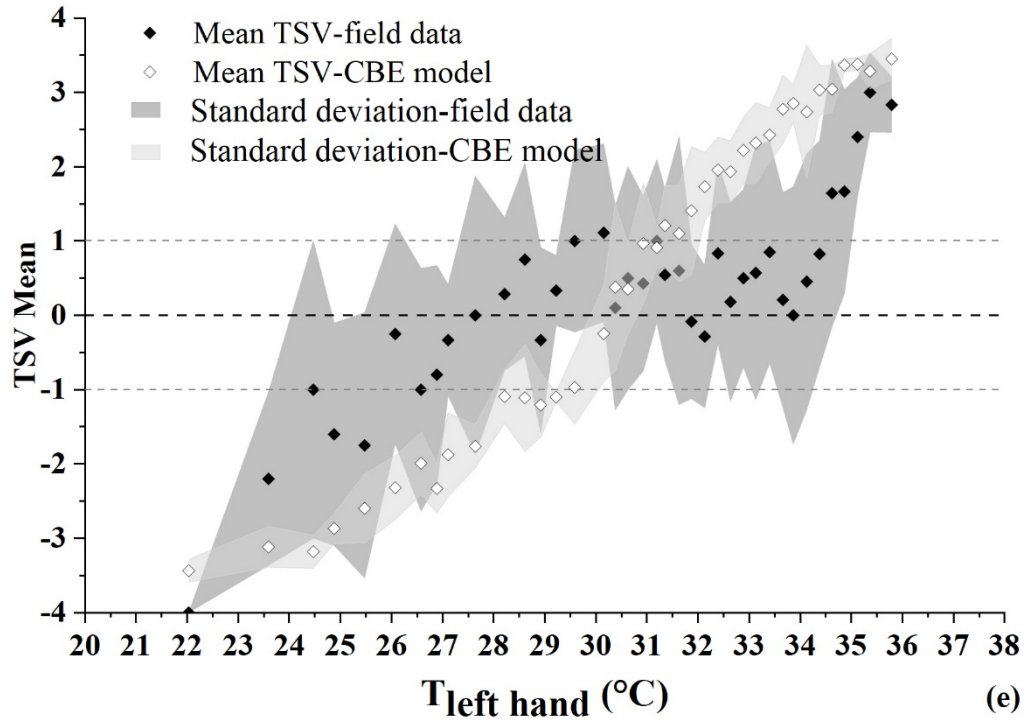
Mean TSV-field data
Mean TSV-CBE model
Standard deviation-field data
Standard deviation-CBE model
TSV Mean
4
3
2
1
0
-1
-2
-3
-4
20 21 22 23 24 25 26 27 28 29 30 31 32 33 34 35 36 37 38
T left hand (°C)
(e)

387

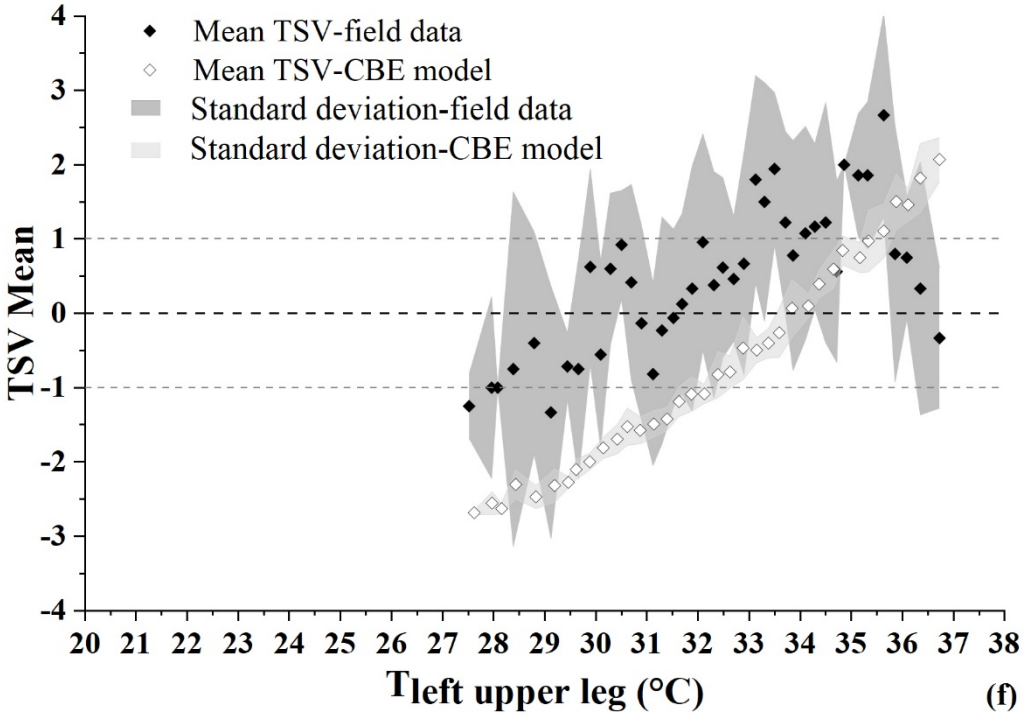
Mean TSV-field data
Mean TSV-CBE model
Standard deviation-field data
Standard deviation-CBE model
TSV Mean
4
3
2
1
0
-1
-2
-3
-4
20 21 22 23 24 25 26 27 28 29 30 31 32 33 34 35 36 37 38
Tleft upper leg (°C)
(f)

388

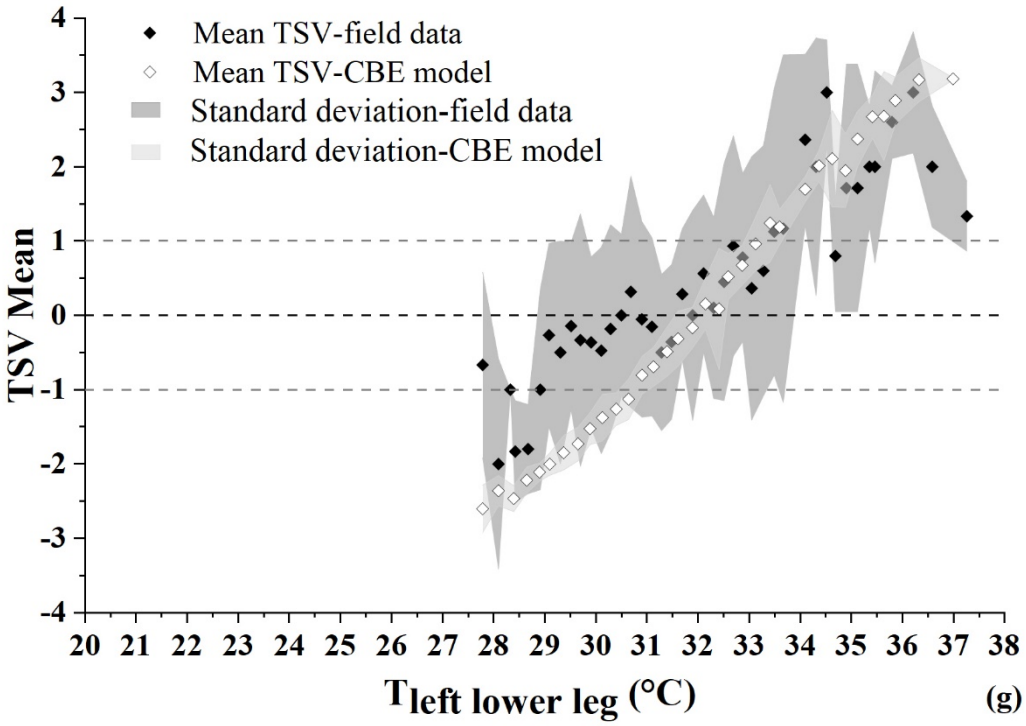
Mean TSV-field data
Mean TSV-CBE model
Standard deviation-field data
Standard deviation-CBE model
TSV Mean
4
3
2
1
0
-1
-2
-3
-4
20 21 22 23 24 25 26 27 28 29 30 31 32 33 34 35 36 37 38
Tleft lower leg (°C)
(g)

389

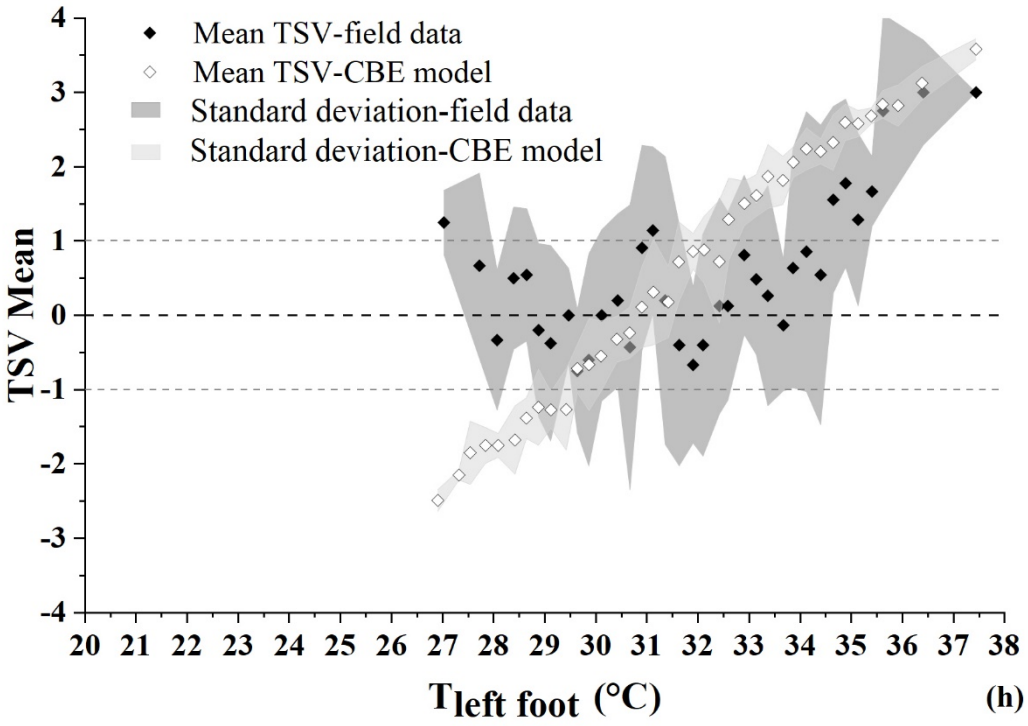

Fig. 6 Correlation between thermal sensation vote (TSV) and skin temperature: (a) between the Overall TSV and Mean skin temperature; and between the local TSV and local skin temperatures: (b) Forehead; (c) Abdomen; (d) Left lower arm; (e) Left hand; (f) Left upper leg; (g) Left lower leg; (h) Left foot.

The measured $T_{skin,m}$ covered the range from 28.0 ℃ to 36.3 ℃. The corresponded $T_{skin,m}$ to the field-surveyed thermal neutral zone was from 29.1 to 34.2 ℃, while that for the simulated data was from 30.9 to 35.1 ℃. The measured $T_{skin,m}$ corresponded to broader thermal neutral status in the surveyed results than the simulated results. Moreover, the field-surveyed thermal neutral range was similar to the range when assuming "TSV=0" as thermal neutral status. The surveyed data points were almost distributed around "TSV = 0" symmetrically in thermal neutral status. When the voted thermal sensation was larger than "TSV = +1", the increasing trend of TSV with the increase of $T_{skin,m}$ was clearer.

Both the $T_{skin,m}$ and overall TSV are the comprehensive indexes of whole-body status, weighted by local body parts. It is needed to observe the relation between local skin temperature and local TSV individually. The temperature ranges of different local body parts vary from each other. The trunk area such as abdomen and forehead had narrower temperature ranges than the extremities. The recorded lowest temperature for abdomen and forehead were 30.0 and 28.5 ℃ respectively. However, take left hand as example for the extremities, its lowest recording was 22.0 ℃.

The relation between the local skin temperature and local thermal sensation varies in different local body parts. As for the abdomen, it was always covered with clothing which is suitable to the weather conditions. Therefore, a wide range of abdomen temperatures corresponded to the

thermal neutral zone (from 29.9 to 35.1 ℃), and no extreme TSV was found. Much different than the surveyed dataset in the abdomen, the CBE-simulated TSV response of the abdomen was close to "cold" (TSV = -3.1) in the lowest measured abdomen temperature and close to "very hot" (TSV = 3.6) in the highest measured abdomen temperature. The surveyed thermal sensation in the forehead was more sensitive to low local skin temperature. However, when the temperature raised to above 31.0 ℃, the thermal sensation entered the thermal neutral zone and stayed there until 34.6 ℃. Compared with the field-measured data, the CBE-simulated TSV did not enter the thermal neutral zone until the forehead temperature raised to 33.9 ℃ then left the thermal neutral zone at 35.1 ℃, making the thermal neutral range in forehead much narrower than the field-surveyed results. These two local body parts in the trunk area, which in total contributed 42% in the calculation of $T_{skin,m}$, all showed a wider local skin temperature range corresponded to the thermal neutral zone from the field measurement.

The extremities, compared with the trunk area, had a much more apparent retention phenomenon of staying in the thermal neutral zone or even staying around the point of "TSV = 0". It is noticeable that the local skin temperature corresponding to the thermal neutral zone become larger when approaching the end of the extremities. Compared to the field-measured data, all the CBE-simulated TSV of the extremities crossed the thermal neutral zone in a straight line. The retention effect during thermal neutrality observed in the field measurement illustrates a need for replacing the set-point with a broader range of data.

3.4 The concept of "null zone" versus "set-point"

The microclimate in the urban environment is known as a highly unstable thermal environment. The relatively short exposure during each survey period enables limited changes in T_{mrt} and T_a, yet the wind environment can change instantly. Unlike the experiment conducted in the controlled climate chamber, the field experiment in the outdoor environment could not control the microclimate variables. Therefore, the field measured skin temperature data in the outdoor environment can illustrate how it reacts and adapts to the continuous fluctuating thermal stimulus.

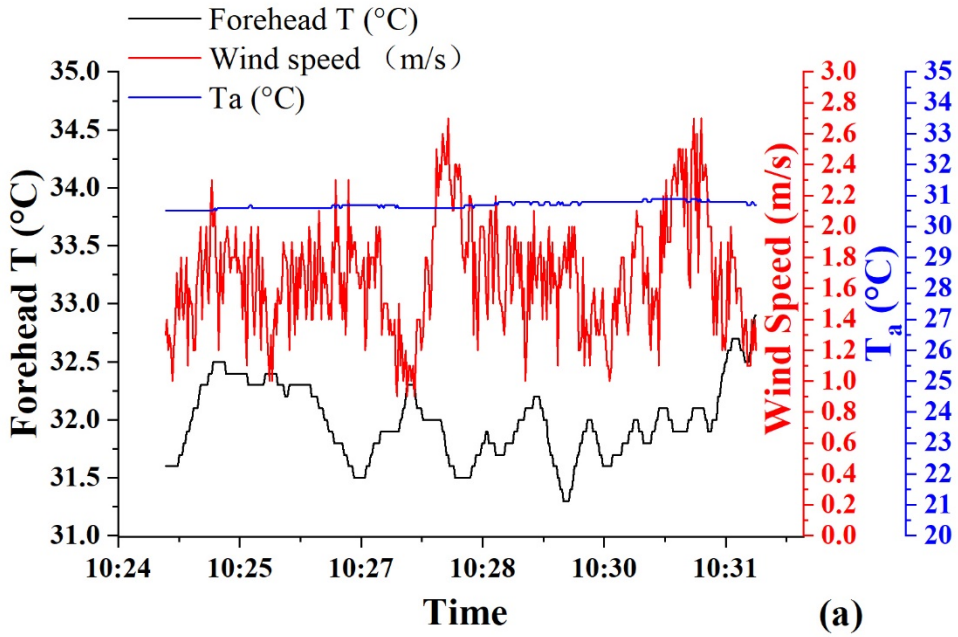

446

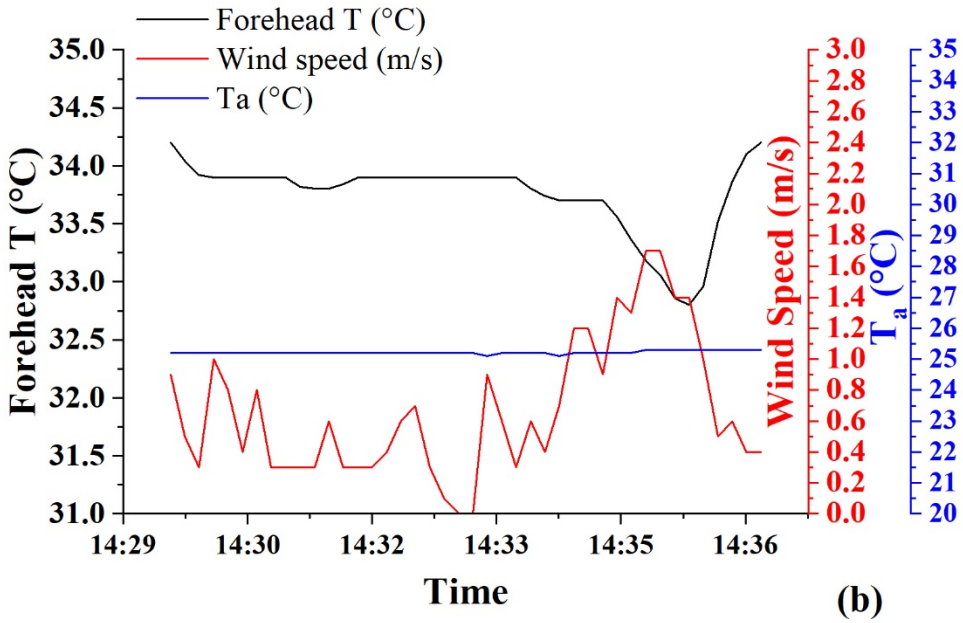

447

448 Fig. 7 Forehead skin temperature change with the change of wind speed (a) continuous
449 sensible wind environment; (b) sudden strong wind environment

450

451 Fig. 7 shows the behavior pattern of the forehead skin temperature with the change of wind
452 speed. The forehead was chosen as an example because it was one of the unclothed body parts.
453 Wind speed in the micro-urban climate was recorded a severe fluctuation during the short-term

experiment exposure. Two typical cases of wind environment were chosen: a continuous sensible wind environment (Fig. 7 (a)) and a suddenly changed wind environment (Fig. 7 (b)). The recorded mean wind speed during the timeslot was about 1.7 m/s for the continuous sensible wind environment (Fig. 7 (a)), and about 0.7 m/s for the case with an immediate changing wind environment. The change of forehead temperature showed an apparent negative correlation with the change of wind speed. As the T_a that day was relatively high at about 30.5 ℃, the range of change of the convective heat loss caused by the change of wind speed was small, and thus the changing range of the forehead temperature was narrow, from 31.3 to 32.9 ℃. For the case of sudden intense wind speed (Fig. 7 (b)), the forehead temperature did not variate much at the beginning as the wind speed kept fluctuating in the low range (under 1.0 m/s). However, when the wind speed suddenly increased from 1.1 m/s to 1.7 m/s, the forehead temperature almost decreased immediately from 33.7 to 32.8 ℃.

It is noticeable that the unclothed skin temperature can have a wide range of variation in the outdoors due to the fluctuating wind environment. The variation range of the local skin temperature depends on the temperature difference between the human body and the outside thermal environment and the strength of the wind speed. Fig. 7 (a) is a typical representative of the continuous changing thermal stimulus in the urban environment. The wind environment in the urban open space kept fluctuating at a certain level. The controlled wind speed of a particular point like the indoor environment is not realistic in the outdoors and thus leads to a doubt of whether the physiological dataset observed in the indoor chamber can represent the real outdoor conditions. Interestingly, corresponding to the continuous changing forehead temperature was the retention effect of the TSV in thermal neutrality, as shown in Fig. 6 (a). The retention effect of the TSV observed in the forehead area showed that human subjects adapt to the continuous disturbance created by the changing wind speed in the urban environment quite well.

In the control theory of thermoregulation, the peripheral thermoreceptors response to both the temperature and the change of temperature [27]. They follow a properties of differential control in dynamic phases (experiencing air temperature change in the climate chamber) while following the properties of proportional control during steady-state [30], which is also applicable to the thermal comfort studies. According to Werner [30], the property of differential control is impossible to be the exclusive control property in the peripheral area, because it only reacts to transient changes of disturbance, but does not counteract to a permanent disturbance. Therefore, proportional control takes the lead when a permanent disturbance happens. The question is whether transient changing wind environment in the outdoors should be treated as a permanent disturbance or a transient disturbance.

The indoor environment has limited air movement and usually can be kept at an unnoticeable level. In that case, a slight increase in wind speed levels can create a thermal sensation difference. Regarding the urban environment, fluctuating wind environment is unavoidable, if wind speed changes in a particular frequency and a certain amplitude, human seems able to adapt to it quickly. As the case in Fig. 7 (a), the wind speed kept changing frequently, but the variation range was kept between 0.9 to 2.7 m/s, no obvious sudden change was observed. Human subjects adapt to such kind of wind environment quite well; thus, we prefer to treat it

as a permanent disturbance. However, when the given wind pattern was destroyed by changing the amplitude or frequency, further thermal sensation difference can be created. The case in Fig. 7 (b) could be an example, within which the wind speed fluctuated at low level (about 0.6 m/s) at most of the time of the experiment period and suddenly increased to a new level (about 1.7 m/s) in a very short period, we prefer to treat it as transient changes of disturbance. This discussion will not be expanded further in this paper, but a proper mathematic description is needed to make a proper description of the disturbance created by different wind environments in the urban setting, and it will be discussed more in our future study. By analyzing the wind environment pattern here, the aim is to bring in the idea that a variability of local skin temperature should be allowed when the urban thermal environment is considered.

Moreover, it is widely accepted that the thermoeffector in thermoregulation reacts proportionally to body temperature. The proportional control works based on the “load error”, which is the deviation of the regulated variable. That means the threshold of the regulated variable determines the output of the regulation and also thermal sensation as a side product. The misconception in thermal comfort research derives from defining the “load error” as the deviation of the body temperature and a fixed “set-point” [22]. If a “set-point” used in the thermal regulation model is applied to the outdoors, it is almost impossible for a human body to remain its thermally stable state. However, the slight fluctuation of the unclothed local skin temperature with the change of wind speed and together with the retention effect shown in the thermal neutral status, indicates that human subjects feel thermally neutral in a certain range instead of a given value. It means either thermal balance could be remained in a range or the thermal sensation feelings be insensitive to a slight fluctuation of thermal imbalance. Therefore, applying set-point in the thermal sensation models cannot accommodate the fluctuation in thermal neutrality, and an inevitable variability should be allowed when the human body is experiencing an outdoor environment. Based on the listed reasons, we proposed using the concept of the "null zone" instead of "set-point” in the thermal regulation model.

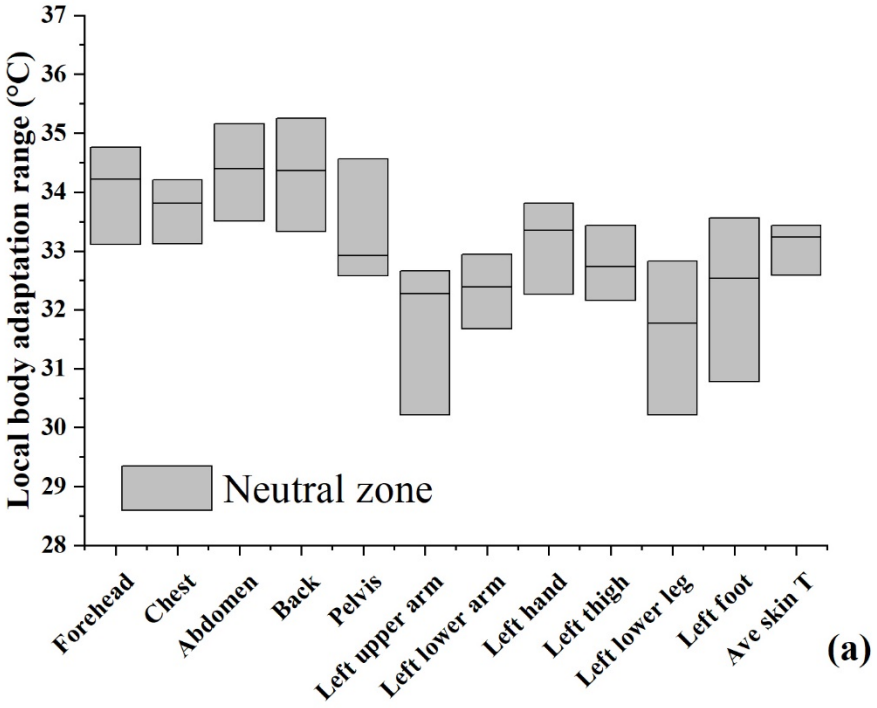
Local body adaptation range (°C)
37
36
35
34
33
32
31
30
29
28
Neutral zone
Forehead
Chest
Abdomen
Back
Pelvis
Left upper arm
Left lower arm
Left hand
Left thigh
Left lower leg
Left foot
Ave skin T
(a)

526

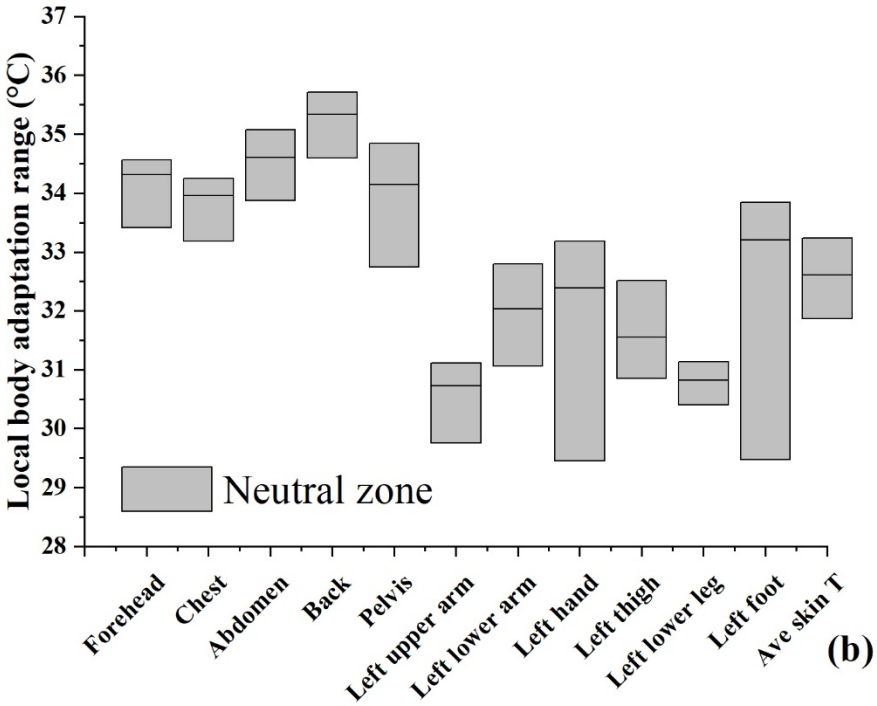
Local body adaptation range (°C)
37
36
35
34
33
32
31
30
29
28
Neutral zone
Forehead
Chest
Abdomen
Back
Pelvis
Left upper arm
Left lower arm
Left hand
Left thigh
Left lower leg
Left foot
Ave skin T
(b)

527

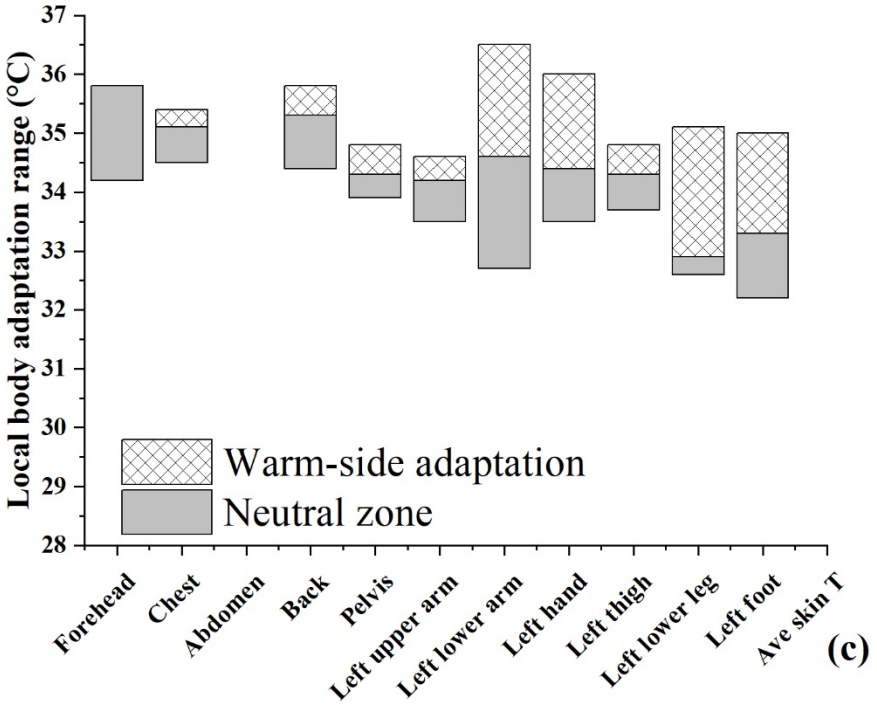

Fig. 8 Local body temperature null zone in thermal neutral status (a) Male; (b) Female (c) thermal adaptation range derived from Zhang's study [37]

The concept of the "null zone" is first defined as a central temperature range associated with limited autonomic regulatory activity [22]. It can also be referred to as "dead band" and "thermoneutral zone". Body temperature fluctuates within this threshold will not trigger further thermoregulation actions [50]. Therefore, the human body can minimize the need for regulatory remediation and thus conserve resources [22]. The "load error" which drives further thermoregulation actions and stronger thermal sensation in this study are defined as the deviation from the thresholds of the null zone. This study will merely discuss the null zone range of local skin temperature; the null zone range of core temperature still needs more data support. The measured local skin temperature data within the null zone was selected by limiting the overall and every local thermal sensation between "-1 to 1", in order to search for the dataset that each local body part and overall thermal sensation feeling are thermal neutral. The filtrated dataset includes 31 human subjects in total, which includes 16 males and 15 females. The local skin temperature null zones are listed in Fig. 8, separating into male and female datasets. The lower and upper limits of the null zone are defined as the value located at the 25% and 75% of the filtrated data in an increasing trend. The medium measured skin temperature values for each local body parts are also shown in Fig. 8 (a, b). The thermal adaptation range in the neutral status and the warm-side adaptation of the CBE model are also reproduced for comparison (Fig. 8 (c)) [37]. The thermal adaptation range in neutral status was obtained from the limited indoor neutral conditions, while the warm-side adaptation range was retrieved from the regression results of the dataset in the extremely hot conditions [37].

Almost all the local body parts for the thermal adaptation range in the CBE model were higher than the field measured null zone results. The reason for that might be due to the difference of dressing pattern: the human subjects joined the CBE experiment wore leotard which was able to tie up the temperature sensors on the skin, while the human subjects for our outdoor experiment wore their own regular clothing. The width of range in the field measured null zone results were much wider than the CBE adaptation range if only focus on its neutral zone; however, if counted in its warm-side adaptation, the width of the field measured and model ranges would be similar. Still, the field measured null zone for the extremities were noticeably lower than the CBE adaptation ranges. The temperature distribution of body parts in the trunk area for male were quite uniform in the range of 33.1 to 35.3 ℃, except for the pelvis where was recorded lower null zone range from 32.6 to 34.6 ℃. The back was recorded as the highest null zone range for females, followed by the abdomen. Forehead and chest recorded similar null zone range. The null zone ranges for pelvis were similar for both males and females. Similar to the adaptation range in the CBE model, the extremities show a much broader null zone range than the trunk parts. The highest value of the extremities for males was recorded as 33.8 ℃ in the left hand while the lowest value was recorded as 30.2 ℃ in both left upper arm and left lower leg. Females had a wider null zone range for the end of the extremities, recorded from 29.4 to 33.2 ℃ for left hand and 29.5 to 33.8 ℃ for the left foot.

The null zone ranges were obtained by limiting the thermal sensation vote, no limitation was added on clothing and environmental conditions, which that ensures the dataset can be applied directly to the real-life outdoor conditions. The thermal neutral range measured in our field study was a comprehensive result of physiological acclimation (adaptation to thermal stimulus), behavioral adjustment (comfortable dressing pattern for different climate conditions), and phycological expectation (willingness for staying in the outdoor environment) [51]. This set of null zone data was used in the further development of the multi-nodal model to replace “set-point”.

3.5 Further development of the multi-nodal model

The further development of the CBE comfort model mainly focuses on two parts: local sensation prediction and selection of dominant local body parts. Equation 7 illustrates the new equation for predicting the static part of a local sensation, which remain using the logistic function of local skin temperature and the original coefficients in the CBE model for local thermal sensation prediction [16] but replacing “set-point” with “null zone”. The null zone results in part 3.4 were used in Equation 7. The coefficients and the logic of the overall thermal sensation prediction still follow the original model (shown in Appendix 1). According to the original model, only the chest, pelvis, abdomen, and back were chosen as the dominant body parts, and such body parts dominant the cool sensation [14]. In the real-life outdoor conditions, such body parts are normally covered with clothing and thus hardly would approach the cold extreme unless local cooling is applied. Compared with the mentioned dominant local body parts, the forehead is normally the unclothed local body part, and it is closed to the body core. Moreover, it showed a strong positive correlation ($R^2 = 96.0\%$) with the overall thermal sensation (shown in Fig. 9). To further confirm our conjecture, the spearman correlation

coefficient r_s was used to measure the correlation strength between the selected local body temperatures and the overall thermal sensation. The absolute value of r_s is between 0 and 1 [52]. The higher the absolute r_s, the stronger the association it is. The r_s results are shown in Table 3. Forehead showed the highest r_s of 0.73 among the other dominant local body parts. This result indicates the importance of the forehead, and thus, it should also be listed as one of the dominant body parts.

$$\text{Local sensation}_{static} = 4\left(\frac{2}{1+e^{[-(C1+K1)\left(T_{skin,i}-T_{skin,i,null\ zone}\right)+K1\left(T_{skin,m}-T_{skin,m,null\ zone}\right)]}} - 1\right)$$

Equation (7)

$$R^2 = 1 - \frac{\sum(Y_{actual}-Y_{predict})^2}{\sum(Y_{actual}-Y_{mean})^2}$$

Equation (8)

Yet this revision focuses only on the relation between the skin temperature and thermal sensation, using skin temperature as the comprehensive parameters of the reflection for the outside thermal environment and personal clothing. The field-surveyed TSV was used to compare with the results from the revised model. We did not separate the original dataset into the dataset for model development and the dataset for verification because the revised model was developed based on merely the measured skin temperature instead of the statistic regression using the subjective voting.

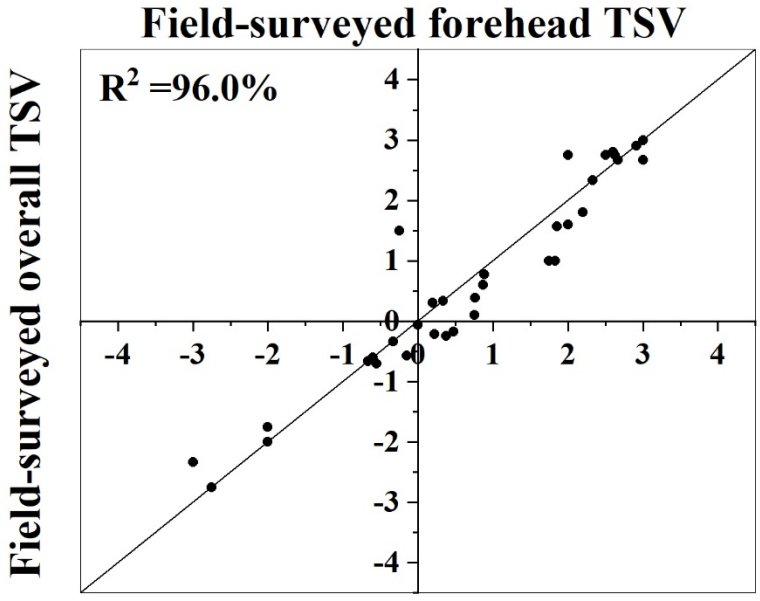

Fig. 9 The relation between field-surveyed forehead TSV and overall TSV

Table 3. Spearman correlation coefficient (r_s) for the correlation between selected local body parts and the overall thermal sensation vote

Local body parts	Forehead	Chest	Abdo	Back	Pelvis
r_s	0.73	0.30	0.66	0.32	0.43

621

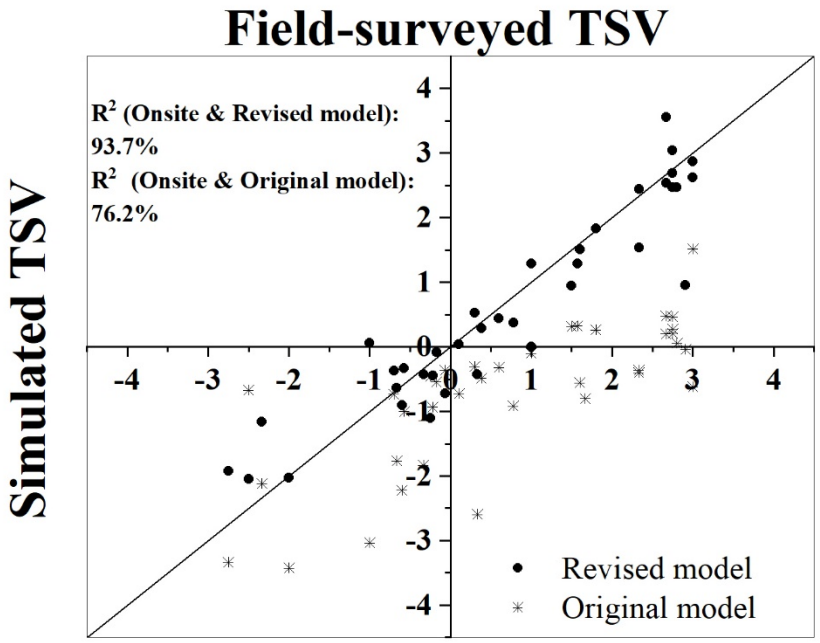

622

623 Fig. 10 Prediction results compared with the field-surveyed data (the revised model vs. the
624 original model)

625

626 Fig. 10 shows the comparison results of the simulated data and the field-surveyed data. Two
627 datasets are shown in Fig. 10: the dataset using the original model framework along with the
628 original CBE thresholds shown in Fig. 8 (c), and revised model along with the dataset using the
629 null zone data (shown in Fig. 8 (a, b)). A 45-degree auxiliary line was added. The data points
630 of the revised model were much closer to the 45-degree line than the simulation data of the
631 original model. As the thresholds for local body parts in the original model were relatively high,
632 the deviations of the measured local body temperature and the upper bound of the threshold
633 were not large and thus very limited data points of the original model located in the hot side.
634 On the contrary, the cold extreme was easy to be approached in this case. R^2 was used to
635 evaluate the performance of the revised model (Equation 8). R^2 of the revised model was
636 93.7%, while that of the original model was 76.2%. An improvement of 17.5% was realized
637 through the revision.

638

639 **4 Conclusions**

640

641 This study focuses on the application of the CBE model in the outdoor environment. A primary
642 comparison of the overall TSV and TCV from the field-collected and the CBE-simulated
643 datasets organized using T_{op} started the discussion. The CBE-simulated TSV was higher than
644 the field-surveyed TSV. The CBE-simulated TCV was mainly located on the uncomfortable

side, while above half of the surveyed TCV was located on the comfortable side. To further locate the problem causing the difference in TSV prediction. A comparison between the field measured, and CBE-simulated mean skin temperature was conducted. A difference exists between the measured and simulated mean skin temperature. Therefore, the measured skin temperature was used as the input in the original CBE comfort model in further analysis to avoid the prediction difference generated by the multi-nodal thermal regulation model. Noticeable retention effect exists in the thermal neutral status of the local body parts when showing the relation between the local and mean body temperatures and field-surveyed TSVs. This phenomenon differs a lot from the CBE-simulated local and overall TSV datasets where "set-point" was applied.

A discussion about the "null zone" and "set-point" was brought forward from two aspects: the adaptation to persistent thermal stimulus and the mechanism of the control theory for temperature regulation. Considered the fluctuating characteristics of the wind environment in the outdoors, it is proposed using the "null zone" instead of "set-point" in the calculation of "load error". A revised definition of "load error" used in thermal comfort studies was proposed as the deviation between the regulated variable and its threshold of null zone. The null zone ranges of skin temperature for different local body parts were defined for the first time in the real-life outdoor environment.

Finally, the CBE comfort model was further developed to fit in outdoor settings. The revision mainly focused on two aspects: applying the measured null zone range in the calculation of local thermal sensation, adding the forehead as one of the dominant body parts when determining overall thermal sensation. About 93.7% of the variation in the field-surveyed overall TSV was addressed by the revised CBE comfort model.

This paper focuses on improving the prediction accuracy of thermal sensation when applying the CBE comfort model in the outdoor conditions where no noticeable temperature change of air temperature and solar radiation. The improvement of the thermal comfort prediction is not the main issue under discussion, and we will address the thermal comfort issue in future studies.

Acknowledgement

The onsite measurements at Sydney, Australia were undertaken under the sponsorship of a PhD student exchange program supported by The Hong Kong Polytechnic University. The assistances from the technical officers Mr Kenny Hung at Hong Kong Polytechnic University and Mr. James Love and Zach Benitez at the University of Sydney in the instrumentation set-up are highly appreciated.

Reference

[1] D. DUNNE, Climate change made Europe's 2019 record heatwave up to '100 times more likely', 2019.

[2] N. Nazarian, J.A. Acero, L. Norford, Outdoor thermal comfort autonomy: Performance metrics for climate-conscious urban design, Building and Environment 155 (2019) 145-160.

[3] M. Aminipouri, D. Rayner, F. Lindberg, S. Thorsson, A.J. Knudby, K. Zickfeld, A. Middel, E.S. Krayenhoff, Urban tree planting to maintain outdoor thermal comfort under climate change: The case of Vancouver's local climate zones, Building and Environment 158 (2019) 226-236.
[4] T. Zölch, M.A. Rahman, E. Pfleiderer, G. Wagner, S. Pauleit, Designing public squares with green infrastructure to optimize human thermal comfort, Building and Environment 149 (2019) 640-654.
[5] A. Ghaffarianhoseini, U. Berardi, A. Ghaffarianhoseini, K. Al-Obaidi, Analyzing the thermal comfort conditions of outdoor spaces in a university campus in Kuala Lumpur, Malaysia, Science of the total environment 666 (2019) 1327-1345.
[6] J. Liu, X. Zhang, J. Niu, K. Tse, Pedestrian-level wind and gust around buildings with a 'lift-up'design: Assessment of influence from surrounding buildings by adopting LES, Building Simulation, Springer, 2019, pp. 1107-1118.
[7] J. Liu, J. Niu, Y. Du, C.M. Mak, Y. Zhang, LES for pedestrian level wind around an idealized building array—Assessment of sensitivity to influencing parameters, Sustainable Cities and Society 44 (2019) 406-415.
[8] Z. Fang, X. Feng, J. Liu, Z. Lin, C.M. Mak, J. Niu, K.-T. Tse, X. Xu, Investigation into the differences among several outdoor thermal comfort indices against field survey in subtropics, Sustainable Cities and Society 44 (2019) 676-690.
[9] T. Sharmin, K. Steemers, M. Humphreys, Outdoor thermal comfort and summer PET range: A field study in tropical city Dhaka, Energy and Buildings (2019).
[10] T. Huang, J. Li, Y. Xie, J. Niu, C.M. Mak, Simultaneous environmental parameter monitoring and human subject survey regarding outdoor thermal comfort and its modelling, Building and Environment 125 (2017) 502-514.
[11] D. Fiala, G. Havenith, P. Bröde, B. Kampmann, G. Jendritzky, UTCI-Fiala multi-node model of human heat transfer and temperature regulation, International journal of biometeorology 56(3) (2012) 429-441.
[12] A.F. Ansys, 14.0 Theory Guide, 2011.
[13] H. Zhang, E. Arens, C. Huizenga, T. Han, Thermal sensation and comfort models for non-uniform and transient environments, part II: Local comfort of individual body parts, Building and Environment 45(2) (2010) 389-398.
[14] H. Zhang, E. Arens, C. Huizenga, T. Han, Thermal sensation and comfort models for non-uniform and transient environments, part III: Whole-body sensation and comfort, Building and Environment 45(2) (2010) 399-410.
[15] Y. Zhao, H. Zhang, E.A. Arens, Q. Zhao, Thermal sensation and comfort models for non-uniform and transient environments, part IV: Adaptive neutral setpoints and smoothed whole-body sensation model, Building and Environment 72 (2014) 300-308.
[16] H. Zhang, E. Arens, C. Huizenga, T. Han, Thermal sensation and comfort models for non-uniform and transient environments: Part I: Local sensation of individual body parts, Building and Environment 45(2) (2010) 380-388.
[17] S. Park, S.E. Tuller, M. Jo, Application of Universal Thermal Climate Index (UTCI) for microclimatic analysis in urban thermal environments, Landscape and Urban Planning 125 (2014) 146-155.
[18] K. Blazejczyk, Y. Epstein, G. Jendritzky, H. Staiger, B. Tinz, Comparison of UTCI to selected thermal indices, International journal of biometeorology 56(3) (2012) 515-535.

[19] Y. Xie, T. Huang, J. Li, J. Liu, J. Niu, C.M. Mak, Z. Lin, Evaluation of a multi-nodal thermal regulation model for assessment of outdoor thermal comfort: Sensitivity to wind speed and solar radiation, Building and Environment 132 (2018) 45-56.
[20] I. Golasi, F. Salata, E. de Lieto Vollaro, M. Coppi, Complying with the demand of standardization in outdoor thermal comfort: A first approach to the Global Outdoor Comfort Index (GOCI), Building and Environment 130 (2018) 104-119.
[21] A.A. Romanovsky, Thermoregulation: some concepts have changed. Functional architecture of the thermoregulatory system, American journal of Physiology-Regulatory, integrative and comparative Physiology 292(1) (2007) R37-R46.
[22] T. Parkinson, R. De Dear, Thermal pleasure in built environments: physiology of alliesthesia, Building Research and Information 43(3) (2015) 288-301.
[23] J. Werner, The concept of regulation for human body temperature, Journal of thermal biology 5(2) (1980) 75-82.
[24] J.A. Stolwijk, A mathematical model of physiological temperature regulation in man, (1971).
[25] J. Werner, Functional mechanisms of temperature regulation, adaptation and fever: complementary system theoretical and experimental evidence, Pharmacology and therapeutics 37(1) (1988) 1-23.
[26] E.A. Arens, H. Zhang, The skin's role in human thermoregulation and comfort, Thermal and Moisture Transport in Fibrous Materials, Woodhead Publishing Ltd2006, pp. 560-602.
[27] H. Hensel, Thermal sensations and thermoreceptors in man, Charles C. Thomas1982.
[28] R. De Dear, Revisiting an old hypothesis of human thermal perception: alliesthesia, Building Research & Information 39(2) (2011) 108-117.
[29] C. Cheng, T. Matsukawa, D.I. Sessler, O. Makoto, A. Kurz, B. Merrifield, H. Lin, P. Olofsson, Increasing mean skin temperature linearly reduces the core-temperature thresholds for vasoconstriction and shivering in humans, The Journal of the American Society of Anesthesiologists 82(5) (1995) 1160-1168.
[30] J. Werner, System properties, feedback control and effector coordination of human temperature regulation, European journal of applied physiology 109(1) (2010) 13-25.
[31] E. Foda, K. Sirén, A new approach using the Pierce two-node model for different body parts, International journal of biometeorology 55(4) (2011) 519-532.
[32] J. Bligh, A theoretical consideration of the means whereby the mammalian core temperature is defended at a null zone, Journal of Applied Physiology 100(4) (2006) 1332-1337.
[33] S.-i. Tanabe, J. Nakano, K. Kobayashi, Development of 65-node thermoregulation-model for evaluation of thermal environment, Journal of Architecture Planning and Environmental Engineering (541) (2001) 9-16.
[34] H. Belding, T. Hatch, Index for evaluating heat stress in terms of resulting physiological strains, Heating, piping and air conditioning 27(8) (1955) 129-36.
[35] K. Brück, E. Baum, H.P. Schwennicke, Cold-adaptive modifications in man induced by repeated short-term cold-exposures and during a 10-day and-night cold-exposure, Pflügers Archiv 363(2) (1976) 125-133.
[36] J. Bittel, Heat debt as an index for cold adaptation in men, Journal of Applied Physiology 62(4) (1987) 1627-1634.
[37] H. Zhang, Human thermal sensation and comfort in transient and non-uniform thermal environments, Center for the Built Environment (2003).

[38] A.V. Bradley, J.E. Thornes, L. Chapman, D. Unwin, M. Roy, Modelling spatial and temporal road thermal climatology in rural and urban areas using a GIS, Climate Research 22(1) (2002) 41-55.
[39] B. Department；, Design and Construction Requirements for Energy Efficiency of Residential Buildings Hong Kong Retrieved fromhttp, 2014.
[40] Y. Xie, J. Liu, T. Huang, J. Li, J. Niu, C.M. Mak, T.-c. Lee, Outdoor thermal sensation and logistic regression analysis of comfort range of meteorological parameters in Hong Kong, Building and Environment (2019).
[41] F. Vignola, J. Michalsky, T. Stoffel, Solar and infrared radiation measurements, CRC press2016.
[42] K. Zonen;, CNR 4 Net Radiometer Instruction Manual.
[43] K.Y. Kondratyev, Radiation regime of inclined surfaces, Unknown (1977).
[44] A.A. Lacis, J. Hansen, A parameterization for the absorption of solar radiation in the earth's atmosphere, Journal of the atmospheric sciences 31(1) (1974) 118-133.
[45] R.J. de Dear, E. Arens, Z. Hui, M. Oguro, Convective and radiative heat transfer coefficients for individual human body segments, International Journal of Biometeorology 40(3) (1997) 141-156.
[46] Y. Yu, J. Liu, K. Chauhan, R. de Dear, J. Niu, Experimental study on convective heat transfer coefficients for the human body exposed to turbulent wind conditions, Building and Environment (2019) 106533.
[47] X. Zhou, H. Zhang, Z. Lian, Y. Zhang, A model for predicting thermal sensation of Chinese people, Building and Environment 82 (2014) 237-246.
[48] Z. Wang, H. Yu, M. Luo, Z. Wang, H. Zhang, Y. Jiao, Predicting older people's thermal sensation in building environment through a machine learning approach: Modelling, interpretation, and application, Building and Environment (2019) 106231.
[49] D. Lai, X. Zhou, Q. Chen, Measurements and predictions of the skin temperature of human subjects on outdoor environment, Energy and Buildings 151 (2017) 476-486.
[50] N. Taylor, J. Werner, I.B. Mekjavic, Concepts in physiological regulation: a thermoregulatory perspective, (2008).
[51] G.S. Brager, R.J. De Dear, Thermal adaptation in the built environment: a literature review, Energy and buildings 27(1) (1998) 83-96.
[52] S. Dowdy, S. Wearden, D. Chilko, Statistics for research, John Wiley & Sons2011.

Appendix

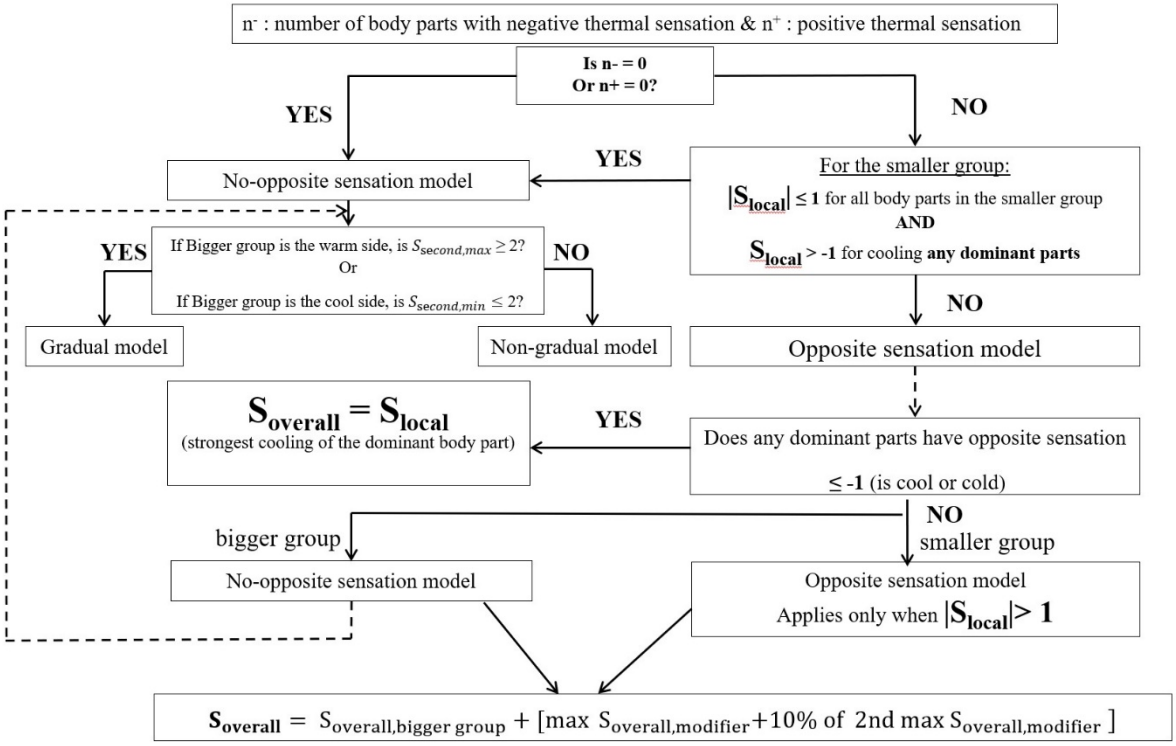

Appendix 1. Schematic diagram of the logic flow in the overall thermal sensation model (reproduced based on the reference [14])